

Fiber Bragg grating based four-bit optical beamformer

Sean Durrant^a, Sergio Granieri^{* a}, Azad Siahmakoun^a, Bruce Black^b

^a Department of Physics and Optical Engineering

^b Department of Electrical and Computer Engineering

Rose-Hulman Institute of Technology, 5500 Wabash Ave., Terre Haute, Indiana 47803, USA

ABSTRACT

In this paper we implement and characterize a two-channel optical programmable beamformer. The system is designed to achieve four-bit resolution. The architecture of the programmable dispersion matrix is based on an array of four delay-lines each having two spliced fiber Bragg gratings. We have experimentally investigated the optical signal processing performance of the optical beamformer in receive and transmit modes. Beampatterns for RF range 40 - 200 MHz are presented along with the theoretical calculations. The main lobe of the beampattern is shown to be independent of frequency for several target positions thus demonstrating a “squint-free” characteristic of this optical processor.

Keywords: Optical signal processing, Phased-array antenna, Fiber Bragg gratings, True-time delay beamforming.

1. INTRODUCTION

Phased array antennas (PAA) along with beamforming systems are widely used in radar, satellite and mobile communication systems. In such RF/microwave systems, including both high-resolution PAA and signal processing electronics, true-time delay (TTD) phase shifters are required. Individual transmit/receive-element control allows the implementation of beam steering and shaping. However, it is desirable that antennas have wide scan angles, wide operational bandwidths and multiple simultaneous independent beams. In conventional RF systems, TTD is achieved by switching between different lengths of electrical cable. However, these implementations tend to be bulky, heavy and susceptible to electromagnetic interference (EMI). Fiber-optic systems provide benefits since the beamforming system becomes smaller and lighter and can be controlled at high speed and it is immune to EMI.

In the last decade, several optical techniques have been proposed for PAA control using fiber-optic systems [1]. In particular, systems using high-dispersion fibers [2-4] and fiber Bragg reflectors [5-7] for providing time delays have been proposed and demonstrated.

In this paper we design and experimentally demonstrate a two-channel true-time delay optical beamformer for controlling a phased array antenna using direct modulation of laser sources. The wideband processor has a resolution of four bits. In section 2 we describe in detail the theory of the beamformer for transmit and receive modes. The beamformer measurements and analysis are discussed in section 3. Concluding remarks are given in section 4.

2. SYSTEM OPERATION

A schematic drawing of the beamformer architecture in the transmit mode is shown in Figure 1(a). Two laser diodes provide optical carriers at λ_1 and λ_2 wavelengths (channels). An RF signal modulates the driving-currents (internal modulation) of the lasers which in turn modulates the optical carriers. RF cables and fiber patch-cords are set

* Corresponding author, phone: 812 877 8080, fax: 812 877 8061, e-mail: granieri@rose-hulman.edu

to ensure zero phase delay between the RF components after optical carriers are coupled. The modulated carrier feeds a programmable dispersion matrix (PDM), which performs the true-time delay processing. For each configuration of the PDM, λ_1 either leads or lags λ_2 by a time-period. At the output of the PDM, after a proper phase difference is set, the channels are de-multiplexed. Two broadband photo-detectors recover the delayed RF signals that are to feed the antenna elements.

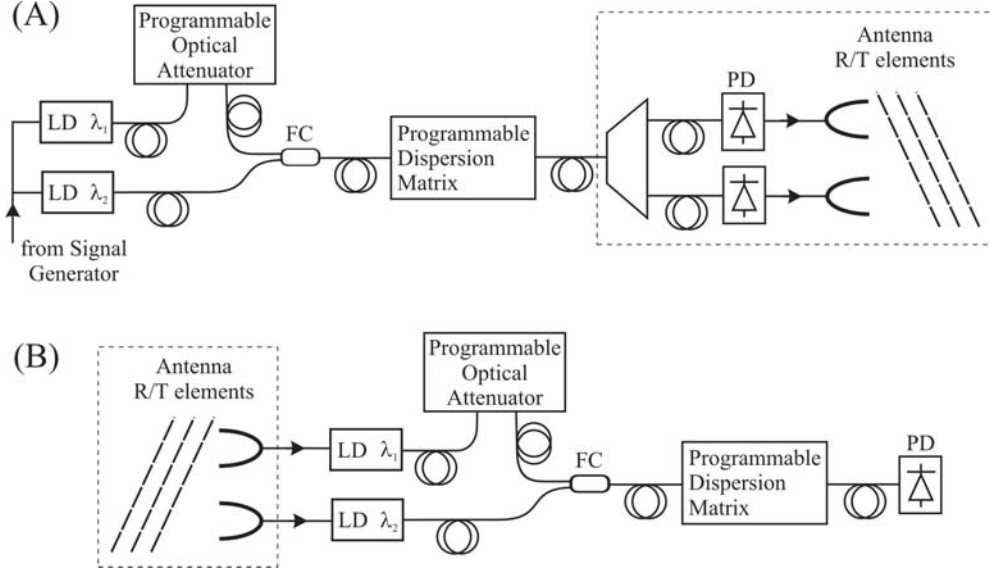


Figure 1: Beamformer setup configuration for: (a) transmit mode and (b) receive mode.

The 4-bit architecture of the PDM, which is based on fiber Bragg grating arrays, is shown in figure 2. The N -bit version of two-channel architecture consists of an array of N delay lines. Each delay line is constructed by splicing two FBG. The center wavelength of each FBG matches one of the multiplexed optical channels. The separation between Bragg reflectors is different for each delay line. Thus, the time delay(s) between channels are proportional to these separations and are binary multiples of the first line (minimum delay time). The separation of two adjacent gratings for the i^{th} line is given by

$$\Delta L_i = 2^{i-1} \Delta L_1, \quad (1)$$

where ΔL_1 is the minimum separation between gratings that corresponds to line 1. Using Eq. (1) the time delay provided by the i^{th} line can be written as

$$\tau_i = \frac{2 n_{eff} \Delta L_i}{c}, \quad (2)$$

where n_{eff} is the effective refraction index of the fiber and c is the speed of light. Each of the 2^N delay configurations of the PDM is an integer multiple, m , of minimum time delay τ_1 . The minimum time delay associated with line 1 is directly related to the angular resolution and the minimum steering angle of any beamformer [8]. The steered angle θ_m is related to a characteristic parameter of the PDM, that is τ_1 , and a geometrical parameter of the antenna, the transmit/receive element spacing Λ , by

$$\theta_m = \arcsin\left(\frac{c m \tau_1}{\Lambda}\right). \quad (3)$$

It is important to note that in the event that the RF frequency changes instantaneously the angular direction of the radiated beam will not drift. This property is also known as “squint free” beamforming.

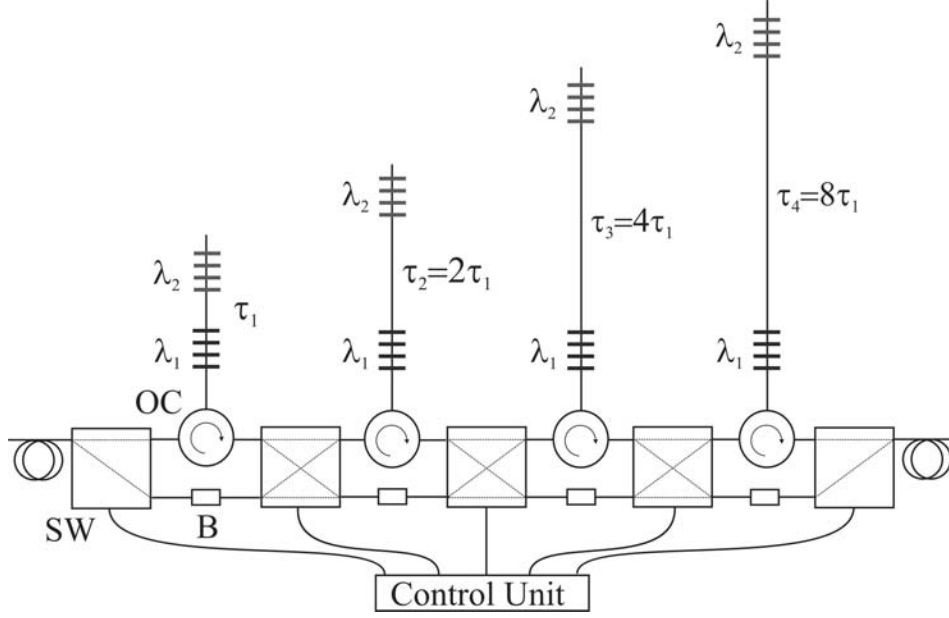


Figure 2: Two-channel 4-bit programmable dispersion matrix. SW: optical switch, B: optical attenuator (balancer), OC: optical circulator.

The schematic for the receive-mode configuration is shown in figure 1(b). An incoming RF signal from a target is received by the two antenna array elements. The phase difference at the antenna elements depends on the target angle. The received RF signal at each element independently modulates one of the optical carriers. The time delay between the multiplexed optical channels is corrected by the PDM and detected with a single photodetector. The output power of the photodetector is a function of the corrected phase difference between the RF signals

$$P(\text{dB}) = 10 \log(K_1 + K_2 \cos \Delta\phi), \quad (4)$$

where $\Delta\phi$ is the phase difference of RF signals and K_1, K_2 are the proportionality constants. Thus, the output power is related to the target angular position via this phase difference. When the PDM properly corrects for the phase difference at the antenna elements, a maximum power will be detected for a given target position.

3. EXPERIMENTAL RESULTS

Our experiments are performed using a 4-bit PDM that provides 16 optical delay configurations. These possible delays are: $\tau_m = m \tau_1$, $m = 0, 1, \dots, 15$. Two 8 mW DFB semiconductor lasers modules, Ortel 1541A, with wavelengths of 1314.3 nm and 1317.1 nm provide the optical carriers. Optical sources are internally modulated with an RF signal of 17 dBm average power. The central wavelengths of the fiber Bragg gratings match the wavelength of optical carriers. All the gratings have reflectivity from 97.7% to 99.8% and FWHM of 0.3 nm to 0.42 nm. As in all delay lines the 1314.3 nm channel lag the 1317.1 nm channel, only asymmetrical beampatterns can be received or

transmitted. That is, the PDM can be programmed to steer only positive or negative angles from antenna broadside [9].

The minimum separation between FBGs is $\Delta L_1 = 0.18$ m corresponding to line 1. Separations in successive lines are: 0.36m, 0.72 m and 1.44 m. The position of FBG is measured with accuracy of ± 2 mm. The theoretical minimum time delay of the PDM, calculated from Eq. (2), is $\tau_1 = 1.76$ ns. Optical circulators are used to route the signals to/from the array lines. In order to get all the delay configurations, two 1x2 and three 2x2 E-Tek optical switches are programmed. The switches are controlled by means of an Agilent 34970A data acquisition unit.

Note that because of the number of components is not the same for each of the paths the optical signals will undergo different levels of attenuation depending on the delay configuration. Thus, as the insertion loss of PDM is path dependent, spurious power variations from changes in constants K_1 and K_2 for different configurations can affect the measurements. In order to balance the optical power in the PDM, in-fiber air-gap mechanical attenuators are placed in each of the paths that bypass the delay lines, as shown in Figure 2. Since the reflectivity of each FBG is different in each line, the optical power output of the PDM is different for each WDM channel. This unbalanced “in-line” power is different for each delay line. To compensate for these changes one of the lasers is coupled to an EXFO FVA3100 programmable optical attenuator. After a complete balancing, the insertion loss of the system is approximately 11.7 dB. The main sources of loss are connectors and optical circulators in the PDM.

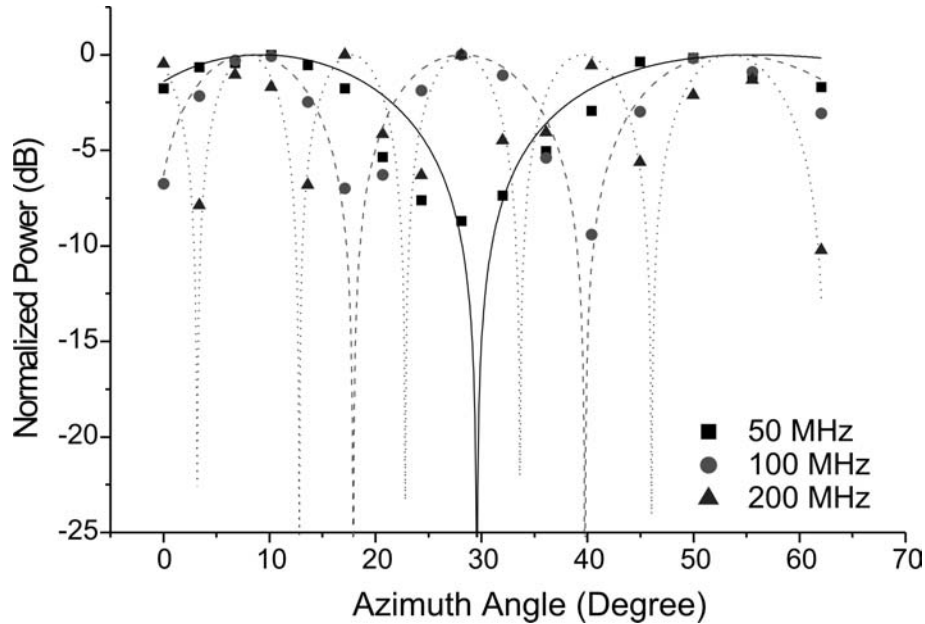


Figure 3: Beam patterns obtained in transmit mode at frequencies 50 MHz, 100 MHz, and 200 MHz.

3.1 Time delay measurements

In order to characterize the time delays produced by the system, the configuration in Figure 1(a) is used. The laser diodes are fed with an RF signal out of port #1 of a vector network analyzer. Port #2 of network analyzer detects the RF signal out of the Thorlabs DC400FC photodetectors, one at a time. Therefore, the phase and magnitude of s-parameter s_{21} are measured for each channel. For a given frequency, the time delay introduced by the PDM can be obtained by subtracting the phase values associated with the parameter S_{21} of the two channels according with $\Delta\phi_m = \phi_0 + 2\pi\nu_{RF}\tau_m$, where $\Delta\phi_m$ is the phase difference for the m^{th} delay configuration, ν_{RF} is the center frequency

of RF, and ϕ_0 is an arbitrary constant phase shift. Experimental data is obtained by sweeping the RF signal of the vector network analyzer between 100 MHz and 1 GHz. The time delay is calculated from the slope of the linear fit to the data. Calculated time delays have errors of less than 1% compared with the expected values. These discrepancies can be attributed to grating spacing errors and phase noise.

3.2 Beampattern characterization

For beampattern measurement and characterization of transmit mode, the configuration shown in Figure 1(a) is slightly modified. The output signal from the PDM is detected by a single photodetector and a Tektronix 2782 RF Spectrum Analyzer. Thus, the RF phase shift created by the PDM is transformed to power variations according to Eq. (4). In order to obtain the transmit beampattern for a desired signal frequency, the PDM is stepped through each of the 16 possible time delay configurations. Figure 3 shows the experimental and theoretical beampatterns for signals at frequencies 50 MHz, 100 MHz, and 200 MHz. These figures illustrate that the beamformer angular steering range is 0° (broadside) to 62° . Theoretical curves are calculated from Eqs. (3) and (4).

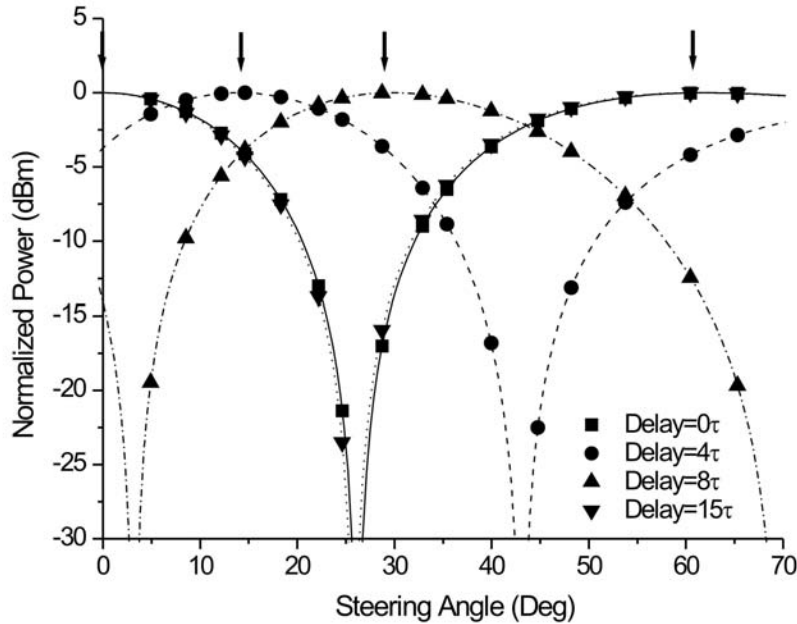


Figure 4: Beampatterns obtained for an incoming RF signal of 40 MHz in receive mode for: no delay, $4\tau_1$, $8\tau_1$, and $15\tau_1$. These cases correspond with optical carriers passing through: none of the delay lines, third delay line, fourth delay line, and all delay lines respectively.

For the receive mode measurements the incoming RF signal from a target is simulated by a HP model 83650A RF synthesizer. The output of the RF synthesizer is split and sent to the laser diodes shown in Figure 1(b). To simulate the phase difference between two antenna elements due to a non-broadside target, an RF phase shifter is introduced before one of the laser inputs. Beampatterns are constructed by sweeping the RF phase shifter and measuring the RF output power from a single photodetector using the RF spectrum analyzer. Figure 4 illustrates typical beam-patterns measured for an incoming RF signal at 40 MHz and four different PDM delay configurations: $m=0$, 4, 8 and 15. Angular position of the main lobe (marked by an arrow) changes with the switch configuration according with Eq.(3). Note that beampatterns for $m=0$ and $m=15$ appear to overlap because the phase difference introduced by the PDM for

$m=15$ at this particular frequency is approximately 2π . Figure 5 shows beam-pattern measurements for three RF signals of 40 MHz, 70 MHz, and 100 MHz. Figure 6(a) corresponds to zero delay, i.e., the optical carriers do not pass through any of the FBG array lines. Hence the target is detected at the broadside position. In figure 6(b) through (d) the carriers pass through different combinations of delay lines in order to provide the desired time delay. In these cases, the PDM is detecting the target at angular positions of 13.62° , 28.11° , and 62.07° . For all the above figures, the experimental data are fit to Eq. (4) by using a nonlinear curve-fit routine. Notice that Eq. (3) suggests that the antenna steering-angle is a function of phase delay and separation of antenna elements but it is independent of the transmitted/received signal frequency. The position of the main lobe in Figure 5 is shown to be independent of frequencies between 40 - 100 MHz demonstrating the “squint-free” characteristic of the system.

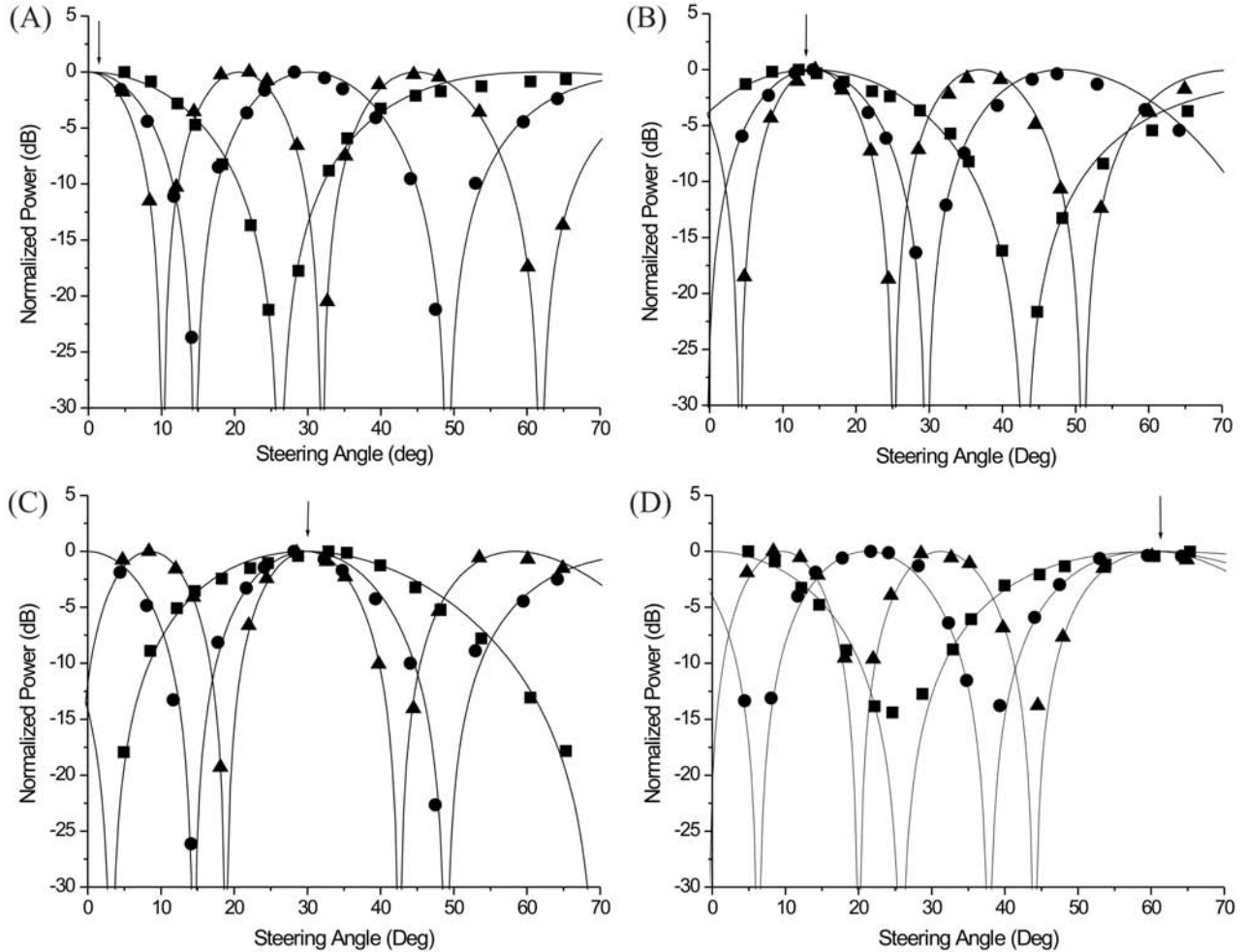


Figure 5: Beam patterns measurement for receive mode at 40 MHz (square), 70 MHz (circle) and 100 MHz (triangle) frequencies for target at angular position of: (a) 0° (broadside), (b) 13.62° , (c) 28.11° , and (d) 62.06° . The main-lobe angular positions, marked by arrows, are independent of RF operating frequencies which confirms a squint-free beamforming.

4. CONCLUSIONS

We have constructed and characterized a 2-channel 4-bit optical beam-former system operating at 1310nm using a fiber-optic programmable dispersion matrix. The working prototype is used to demonstrate the accuracy of generated beam-patterns in the transmit and receive modes for the RF range of 40-200 MHz. Beam patterns are obtained for

steering angles up to 62° . Theoretical and experimental values for main-lobes for different delay configurations are in good agreement. Our optical beamformer exhibits squint-free radiation pattern in RF band of 40-100 MHz. Measurements are limited to 100 MHz in order to obtain a reasonable number of data points per beam lobe. Otherwise, the upper limit is set by the 2 GHz bandwidth of the photodiode. The optical processor can be easily scaled for a large number of antenna elements. Additional channels require only stacking up the same number of FBGs on each array. While improving system resolution to N -bit will require N arrays of FBGs.

ACKNOWLEDGMENTS

The authors would like to acknowledge Daniel Purdy of Office of Naval Research for his support of this project under the contract number N00014-00-1-0782.

REFERENCES

1. N. Riza, Ed., *Selected papers on photonic control systems for phased array antennas MS-136*, SPIE Milestone Series, Washington, 1997.
2. R. Soref, "Optical dispersion technique for time-delay beam steering", *Applied Optics*, **31**, 7395-7397, 1992.
3. R. Esman, M. Frankel, J. L. Dexter, L. Goldberg, M. G. Parent, D. Stilwell and D. G. Cooper, "Fiber-optic prism true time-delay antenna feed", *IEEE Photon. Technol. Lett.*, **5**, 1347-1349, 1993.
4. S. T. Johns, D. A. Norton, C. W. Keefer, R. Erdmann and R. Soref, "Variable time delay of microwave signals using high dispersion fibre", *Electronics Letters*, **29**, 555-556, 1993.
5. R. Soref, "Fiber grating prism for true time delay beamsteering", *Fiber and Integrated optics*, **15**, 325-323, 1996.
6. H. Zmuda, R. Soref, P. Payson, S. Johns and E. Toughlian, "Photonic beamformer for phased array antennas using a fiber grating prism", *IEEE Photon. Technol. Lett.*, **9**, 241-243, 1997.
7. D. Tong, and M. Wu, "Programmable dispersion matrix using Bragg gratings for optically controlled phased array antennas", *IEEE Photon. Technol. Lett.*, **10**, 1018-1020, 1996.
8. B. Black, A. Siahmakoun, L. Slaybaugh, J. Chestnut, and D. Thelen, "Component-level simulation of optical beamforming systems *Proc. SPIE* **4532** 494-9, 2001.
9. S. Palit, S. Granieri, A. Siahmakoun, B. Black, K. Johnson and J. Chestnut, "Binary and Ternary architectures for a two-channel optical receive beamformer" *Technical Digest of International topical meeting on microwave photonics (MWP)*, 273-6, IEICE Electronics Society, Awaji, 2002